

Adsorption of glutamic acid from aqueous solution with calcined layered double Mg–Fe–CO₃ hydroxide

Fei-peng JIAO, Li SHUAI, Jin-gang YU, Xin-yu JIANG, Xiao-qing CHEN, Shao-long DU

School of Chemistry and Chemical Engineering, Central South University, Changsha 410083, China

Received 27 June 2012; accepted 9 January 2013

Abstract: Layered double Mg–Fe–CO₃ hydroxide (Mg–Fe–LDH) with a mole ratio of Mg to Fe of 3 was synthesized by coprecipitation method and calcined product Mg–Fe–CLDH was obtained by heating Mg–Fe–LDH at 500 °C for 6 h. The as prepared Mg–Fe–LDH and calcined Mg–Fe–CLDH were used for removal of glutamic acid (Glu) from aqueous solution, respectively. Batch studies were carried out to address various experimental parameters such as contact time, pH, initial glutamic acid (Glu) concentration, co-existing anions and temperature. Glu was removed effectively (99.9%) under the optimized experimental conditions with Mg–Fe–CLDH. The adsorption kinetics follows the Ho's pseudo second-order model. Isotherms for adsorption with Mg–Fe–CLDH at different solution temperatures were well described using the Langmuir model with a good correlation coefficient. The intraparticle diffusion model fitted the data well, which suggests that the intraparticle diffusion is not only the rate-limiting step.

Key words: calcined layered double hydroxides; glutamic acid; adsorption

1 Introduction

Glutamic acid (Glu) is an amino acid that is widely used in many fields, such as food, drugs, dietary supplements, cosmetics, personal care products and fertilizers [1]. The global demand of Glu is 1.7×10^6 t/a, and China demands roughly 1.1×10^6 t/a [2]. However, most producers do not treat the waste water which contains un-neglected amount of Glu. Nevertheless, Glu is an environmental pollutant as it induces eutrophication and increases BOD/COD value in water [3]. To improve the efficiency of treatment for removing amino acids from waste waters, some measures are available in Refs. [4,5]. However, the adsorption technique is particularly gaining popularity considering its simplicity, versatility and potential for regeneration [6]. Many studies have been reported for adsorption of amino acids on various materials including active carbon, coal, agricultural wastes, wood wastes and clay materials [7,8]. Among them, a class of anionic clay known as layered double hydroxides (LDHs) has been proved to be effective adsorbents for removal of a variety of anionic pollutants.

The general formula of LDHs is

$[M_{1-x}^{II}M_x^{III}(\text{OH})_2]^{x+}A_{x/n}^{n-} \cdot m\text{H}_2\text{O}$, where M^{II} is a divalent metal cation (Mg²⁺, Zn²⁺, etc.); M^{III} is a trivalent metal cation (Al³⁺, Fe³⁺, etc.) that occupies octahedral sites in the hydroxide layers; Aⁿ⁻ is a exchangeable interlayer anion; x is the $n(\text{M}^{III})/[n(\text{M}^{II})+n(\text{M}^{III})]$ that determines the layer charge density. The calcined LDH, denoted as Mg–Fe–CLOH, has a so-called “memory effect” property [9]. This effect makes the formation of M^{II}M^{III}O solid solution in the CLDH capable of recovering the LDH layered structure during treatment of water or aqueous solution containing various anions. When the LDHs are heated above 400 °C, the interlayer CO₃²⁻ can be removed and the resulting CLDH can be used for removing organic anions by either adsorption on the external surface of the layers, or intercalation process and reconstruction behavior. Among these layered compounds, the most studied ones are the aluminum-based materials, such as Mg–Al and Zn–Al [10,11]. However, the presence of Al may have a serious drawback when used in the drinking water treatment. Al exposure has been pointed out as a potential risk factor for the development or speeding up of the Alzheimer syndrome in human being [12]. Considering this scenario, a new material free from toxic metals is required.

Previous studies have been focused on the removal

of Glu by the Mg–Al–CO₃ LDH [13,14]; less attention has been paid to the efficiency removal of Glu by the calcined Mg–Fe–CO₃ LDH, denoted as CLDH. CLDH was selected for adsorption of Glu because most of the aqueous Glu species are anions. The present study aims at investigating the adsorption capacity of Glu on Mg–Fe–CLDH in aqueous medium as a function of various adsorption parameters, such as contact time, pH, initial Glu concentration, co-existing anions and temperature. The equilibrium isotherm and kinetic model for the adsorption process were also studied to evaluate the viability and effectiveness of the process.

2 Experimental

2.1 Preparation of Mg–Fe–LDH and Mg–Fe–CLDH

Mg–Fe–LDH was prepared by the coprecipitation method [15]. A metal salt solution containing MgCl₂·6H₂O (0.15 mol) and FeCl₃·6H₂O (0.05 mol) was added to a vigorously stirred aqueous alkali solution of 0.45 mol of NaOH and 0.15 mol of Na₂CO₃. Both solutions were prepared by using 150 mL deionized water. The pH value of the mixed solution was maintained at slightly higher than 9 with NaOH (0.1 mmol/L). After heating at 80 °C for 24 h, the solid phase was separated from liquid phase by centrifugation and washed thoroughly with deionized water until the pH value was 8.0. Subsequently, the obtained precipitate was dried at 80 °C overnight. Mg–Fe–CLDH was obtained by calcining Mg–Fe–LDH in a muffle furnace at the designated temperature of 500 °C for 6 h.

2.2 Adsorption experiments

A temperature-controlled shaker bath (tolerance: ±0.5 °C) was used for the equilibrium studies. The adsorption experiments were carried out in 250 mL sealed conical flasks. The flasks were placed into the shaker bath immediately after mixing a 50.0 mL Glu solution of appropriate concentration and prearranged amount of Mg–Fe–CLDH. 2 mL samples were extracted at selected time intervals, separated by filtration (using a membrane filter with a pore size of 0.45 μm) and conserved in the vial for latter detection. The concentrations of Glu remaining in solution were then analyzed by ninhydrin colorimetric analysis on a spectrophotometer (UV–9600), and the absorbance was measured at 568 nm.

The quantity of Glu adsorbed by 1 g of Mg–Fe–CLDH at time t , q_t , and the removal rate of Glu were calculated using the following equation:

$$q_t = \frac{(c_0 - c_t)V}{m} \quad (1)$$

$$R = \frac{c_0 - c_t}{c_0} \times 100\% \quad (2)$$

where m is adsorbent mass; V is the suspension volume; c_0 and c_t are the initial concentration and equilibrium concentration of the Glu in solution, respectively

2.3 Analytical methods

Mg–Fe–LDH and Mg–Fe–CLDH before and after the adsorption of Glu (reconstructed Mg–Fe–LDH) were characterized by several techniques. The powder X-ray diffraction (XRD) patterns were recorded on a powder X-ray diffractometer (Rigaku Rint 6000), using Ni-filtered Cu K_α ($\lambda=1.5406$ Å) radiation at voltage of 40 kV and current of 250 mA. Fourier transform infrared spectra (FT-IR) were collected with a Nicolet Avatar360 spectrophotometer (AVATAR 360, Nicolet, USA). Low-temperature N₂ adsorption-desorption experiments were carried out using a Quantachrome Autosorb-1 system. The surface areas of the Mg–Fe–LDH and Mg–Fe–CLDH were calculated using the BET method. Thermal gravimetric analyses DSC–TG measurements were conducted on a STA449C thermal analyzer under atmosphere with a heating rate of 10 °C/min from 25 °C to 800 °C. Elemental analyses for C, H, N in samples were carried out with CHNS analyzer (VarioELIII). Elemental analyses for metal ions in samples were performed using a IRIS Advantage 1000 ICP-AES after the samples were dissolved using dilute HNO₃ (1:1).

3 Results and discussion

3.1 Characterization of Mg–Fe–LDH and Mg–Fe–CLDH

The XRD patterns of Mg–Fe–LDH and Mg–Fe–CLDH are shown in Fig. 1. By analyzing the XRD

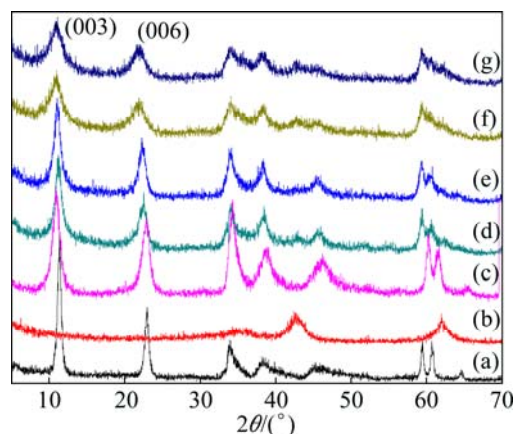


Fig. 1 XRD patterns of Mg–Fe–LDH (a), Mg–Fe–CLDH (b) and reconstructed by Mg–Fe–CLDH in solutions containing Glu with various initial concentrations of 0 mg/L (c), 50 mg/L (d), 100 mg/L (e), 200 mg/L (f) and 500 mg/L (g)

pattern of the synthesized Mg–Fe–LDH, we obtained that the sharpness values of the (003) and (006) peaks demonstrate layered structure of the sample, which agrees well with the previous research. After calcination, the (003) and (006) reflections practically disappear, indicating that the Mg–Fe–LDH structure is destroyed. Only few diffused peaks at 42.38° and 61.98° are observed, which are attributed to MgO (Fig. 1(b)). After Glu removal of 96.2% with Mg–Fe–CLDH at initial Glu concentration of 100 mg/L, there is no significantly difference in the basal spacing of 7.94 \AA (Mg–Fe–LDH) (Fig. 1(a)), which indicates that there are few Glu anions between the interlayer due to the strong interaction of CO_3^{2-} and the layers. Therefore, the Glu adsorption occurred mainly on the external surface of the material. Similar results have been reported for the adsorption of Glu in Mg–Al– CO_3 LDH [13].

The FT–IR analysis from Fig. 2 shows the presence of Glu in the Mg–Fe–LDH, by the increase in the two bands related to the asymmetric and symmetric stretches of the carboxylate group at 1576 cm^{-1} and 1427 cm^{-1} , respectively. Moreover, one band mainly related to the C=O stretching vibration, N–H bending vibration and C–N bending vibration appeared at 1650 cm^{-1} [16], which indicates that the adsorption is successful.

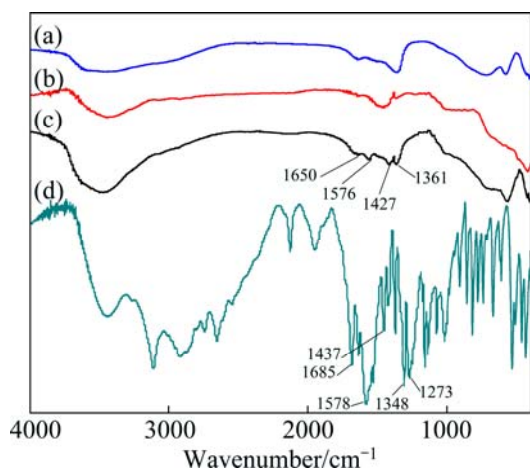


Fig. 2 FT–IR spectra of Mg–Fe–LDH (a), Mg–Fe–CLDH (b), reconstructed Mg–Fe–CLDH at initial Glu concentration of 100 mg/L (c) and Glu (d)

The TG–DSC curves for Mg–Fe–LDH and reconstructed Mg–Fe–LDH are shown in Fig. 3. The TG plot for Mg–Fe–LDH sample shows two steps of mass loss in Fig. 3(a). The mass loss (17.4% of the total mass) in the first step ($50\text{--}240^\circ\text{C}$) with an endothermic peak at 201°C in the DSC curve is attributed to removal of water physisorbed on the external surface of the crystallites. The second mass loss (25.6% of the total mass) occurring between 240°C and 430°C involves dehydroxylation of the layers and loss of volatile species (CO_3^{2-}) arising from the interlayer anions [17]. The TG

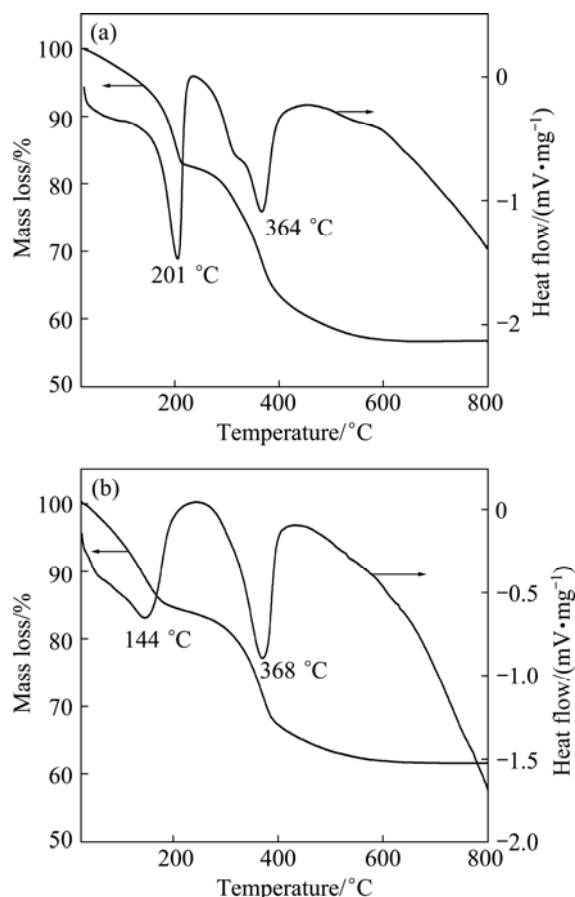


Fig. 3 TG–DSC curves for Mg–Fe–LDH (a) and reconstructed Mg–Fe–LDH (b)

curve for reconstructed Mg–Fe–LDH at initial Glu concentration of 100 mg/L (Fig. 3(b)) also shows two mass loss steps and the mass loss rates are 16.0% and 22.3% in the temperature ranges $50\text{--}250^\circ\text{C}$ and $250\text{--}420^\circ\text{C}$, respectively. Interestingly, the first corresponding event in the DSC curve occurs near 144°C which is lower than that of pure LDH, suggesting the decreased interaction of water molecules with the LDH surface. The reason may be explained that there are weaker interaction between the water molecules and preferential adsorption of Glu anions on the external surface of Mg–Fe–LDH, which indicates the presence of Glu on Mg–Fe–LDH surface. On the basis of the data of thermal analysis and elemental analysis, Mg–Fe–LDH was assigned to the following chemical formula: $\text{Mg}_{0.168}\text{Fe}_{0.056}(\text{CO}_3)_{0.049}(\text{OH})_{0.407}\cdot 0.199\text{H}_2\text{O}$.

The large surface area of adsorbent is in favor of physical adsorption. Therefore, the surface areas of Mg–Fe–CLDH and Mg–Fe–LDH were calculated using the BET method to be 136.62 and $77.91 \text{ m}^2/\text{g}$, respectively. The higher surface area of Mg–Fe–CLDH can be ascribed to the additional mesoporous region, which is formed by the channels and pores after the removal of water and carbon dioxide.

3.2 Adsorption

3.2.1 Effect of pH

Since the pH of the Glu solution plays an important role during the whole adsorption process, the adsorption of Glu by Mg–Fe–CLDH was studied at different initial pH values ranging from 2.0 to 10.0 at temperature 25 °C, and the results are shown in Fig. 4. It can be seen that removal rate of Glu increases with pH and reaches a maximum at pH of 3.8. Near the isoelectric point ($pH_{pzc}=3.32$), the decrease of the adsorption can be attributed to the decrease of the stability of the LDH structures.

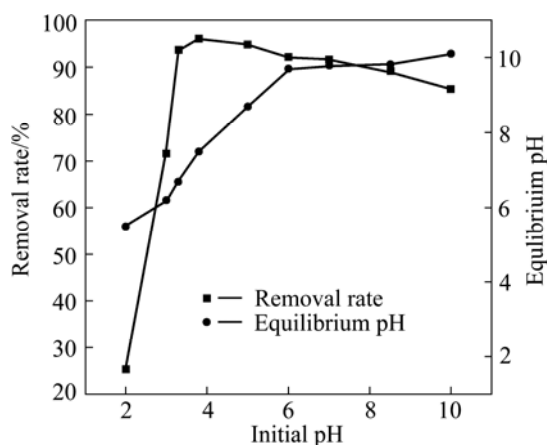


Fig. 4 Effect of initial pH on Glu removal with Mg–Fe–CLDH and on equilibrium pH

When the pH decreases to 3 by addition of hydrochloric acid concentration (HCl), a part of the metal cations in the Mg–Fe–CLDH probably were dissolved. With the increase of pH, Glu molecules change from the univalent positive charge (Glu^+) to divalent negative charge (Glu^{2-}), which is more likely to be loaded onto the positive charged layers of Mg–Fe–LDH. The possible reasons for a decrease at higher pH are the competition of OH^- and the enhanced electrostatic interaction between Glu molecules. At higher pH, the concentration of carbonate ions would increase by addition of an alkaline solution (NaOH). The higher concentrations of OH^- anions and CO_3^{2-} anions at the Mg–Fe–CLDH/water interface lead to a diffusion hindrance of Glu molecules. Consequently, the Glu solution with pH close to 3.8 was applied to the adsorption experiments else without further adjustment.

We found that the initial pH has a small effect on the removal of Glu, due to the enhanced final pH value when the initial pH value was relatively low; for the initial pH 3.0, it would shoot up to 6.2 after the adsorption for 21 h, and the difference between the values of initial and equilibrium pH is shown in Fig. 4. The buffering ability can be explained by the release of OH^- during the rehydration of Mg–Fe–CLDH and the

dissolution of Mg–Fe–LDH at low pH. The insignificant change in the removal rate in the pH range of 3.0–8.5 may be attributed to the buffering ability. The Mg–Fe–CLDH shows a high removal rate over a wide initial pH range of 3.0–8.5, suggesting that it could be potentially applied in different pH systems.

3.2.2 Effect of initial Glu concentration

The effect of contact time (up to 21 h) at varying initial concentrations (50–200 mg/L) of Glu was investigated at 25 °C. In Fig. 5(a), the adsorption capacity of Glu increases with the contact time for any initial Glu concentration; meanwhile, the equilibrium time becomes longer at a higher initial Glu concentration. It can be observed the maximum equilibrium adsorption capacities of 14.9, 24.9, 49.3, 71.6 and 82.6 mg/g at Mg–Fe–CLDH of 2 g/L for 30, 50, 100, 150, 200 mg/L of initial Glu concentration, respectively. Clearly, the equilibrium adsorption capacity of Glu increases with the increase of initial Glu concentration. At higher concentrations, the higher equilibrium adsorption capacity increases due to an increased ratio of initial number of moles of Glu to the available surface areas. Figure 5(b) shows that Glu was almost complete in a short time at low initial Glu concentrations (30, 50, 100 mg/L), suggesting the possibility of the formation of

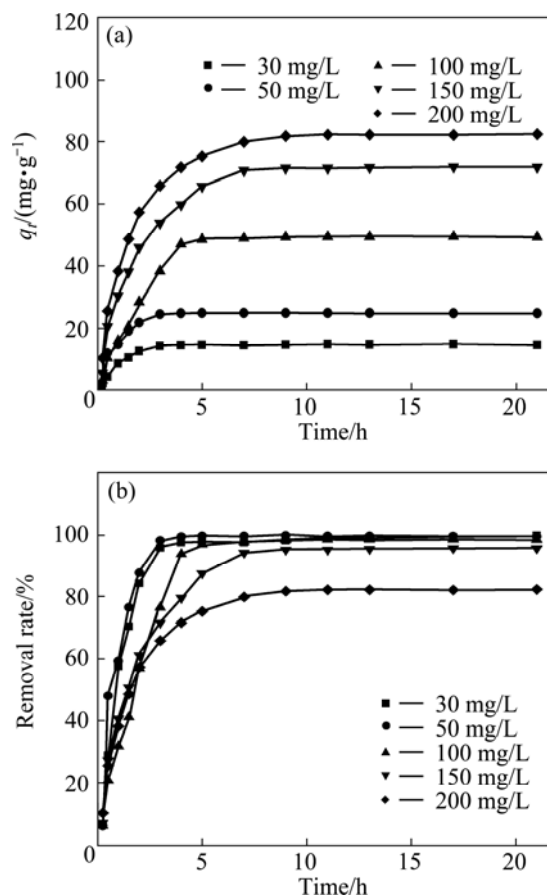


Fig. 5 Effect of contact time at varying initial concentrations on Glu removal with Mg–Fe–CLDH

monolayer coverage of Glu at the outer interface of Mg–Fe–CLDH. However, the removal rate of Glu begins to decline at the initial Glu concentration of 150 mg/L, owing to the limitation of adsorbent dose. The higher initial Glu concentration may have an adverse effect on the external diffusion which improves the intraparticle diffusion rate [18]. Therefore, considering both of the removal efficiency and the adsorption capacity, the subsequent adsorption experiments were performed at the initial Glu concentration of 100 mg/L when the dose of Mg–Fe–CLDH was 2 g/L.

In order to study further the influence of different initial Glu concentration, the XRD patterns of reconstructed Mg–Fe–LDH at different initial concentrations (0, 50, 100, 200 and 500 mg/L) are shown in Fig. 1. It can be observed that the peak intensity decreases and the peak width increases with the increase of initial Glu concentration, reflecting a fall in the crystallinity of the material at a higher initial concentration. The reason may be that the number of intercalated carbonic anions decreases with the increase of initial Glu concentration, which is adverse to the rehydration. However, no evident change in the interlayer spacing was observed ($d_{003}=7.89 \text{ \AA}$ at initial Glu concentration, 0 mg/L and 8.17 \AA at initial Glu concentration of 500 mg/L), indicating that the Glu was adsorbed on the external surface of the Mg–Fe–CLDH rather than intercalated between the interlayers.

3.2.3 Effect of competitive anions

Considering the potential interference, the effects of competing anions were studied and summarized in Fig. 6. Our studies argue that the presence of competing anions clearly affected adsorption efficiencies. In our study, various competing anions were taken at equal concentrations to that of Glu solution (100 mg/L). The interfering effect of all the anions increased with their concentrations. Among all the anions, PO_4^{3-} had the most significantly adverse effect on Glu adsorption,

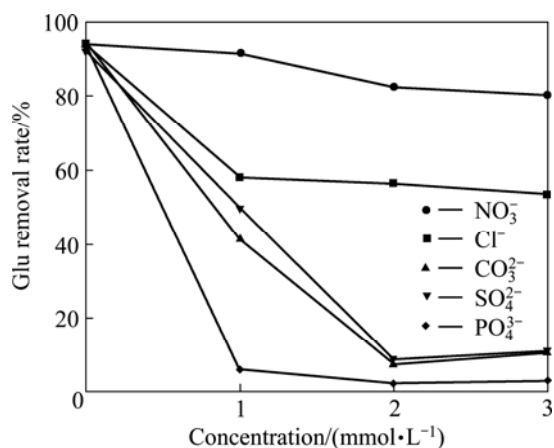


Fig. 6 Effect of competitive anions on removal of Glu by Mg–Fe–CLDH

whereas NO_3^- showed the least effect. The removal rate of Glu followed the order, $\text{PO}_4^{3-} < \text{CO}_3^{2-} < \text{SO}_4^{2-} < \text{Cl}^- \ll \text{NO}_3^-$. Clearly, anions with higher charge density and smaller radius have greater affinities to Mg–Fe–CLDH when these anions are co-existing [19]. Our result coincides with the z/r (charge/radius) comparison, CO_3^{2-} ($2/1.36 \text{ \AA}$) $>$ SO_4^{2-} ($2/2.40 \text{ \AA}$) $>$ Cl^- ($1/1.81 \text{ \AA}$) \gg NO_3^- ($1/2.81 \text{ \AA}$) [19].

3.2.4 Effect of temperature on kinetics

Since temperature is a highly significant parameter in the adsorption process, the kinetics for removal of Glu at different temperatures was studied and two commonly used models were applied to fitting the experiment results: 1) Lagergren's first-order kinetic model (Eq.3) and 2) Ho's pseudo second-order model (Eq. (4)). Both of the equations in linear forms are expressed as follows [20]:

$$\ln(q_e - q_t) = \ln q_e - k_1 t \quad (3)$$

$$\frac{t}{q_t} = \frac{1}{k_2 q_e^2} + \frac{t}{q_e} \quad (4)$$

where q_e is the adsorption capacity of the adsorbate at equilibrium; k_1 and k_2 are the rate constants of pseudo first-order and pseudo second-order adsorption, respectively.

Figure 7 shows that the two fitted kinetic models under different isothermal conditions. The pseudo second-order kinetic model fits the experimental data better, indicating that the rate-limiting step is a chemical adsorption process between Glu and the Mg–Fe–CLDH [21]. Meanwhile, the first-order kinetic model only fits well the experimental data at 25 °C but not others at higher temperatures. The depletion rate of Glu at different temperatures showed that the Glu removal by Mg–Fe–CLDH was enhanced by raising the temperature (see Table 1).

The intra-particle diffusion model known as the Weber and Morris model is expressed by the following equation [22]:

$$q_t = k_p t^{1/2} + C \quad (5)$$

where k_p is the intra-particle diffusion rate constant and can be obtained from the slope of the plot of q_t versus $t^{1/2}$; C is related to the thickness of the boundary layer.

The relationships between q_t and $t^{1/2}$ at different temperatures are given in Fig. 8. It is clear from the figure that the removal of Glu by Mg–Fe–CLDH occurs in three different steps as the plot contains two different straight lines. The first line from 0 to 3 h is attributed to the fast diffusion of the Glu molecules from the aqueous phase to the Mg–Fe–CLDH surface. The second line from 3 h to 8 h is due to the intra-particle diffusion. As can be seen from Fig. 8, the line in the initial stage does not pass through the origin, indicating that the

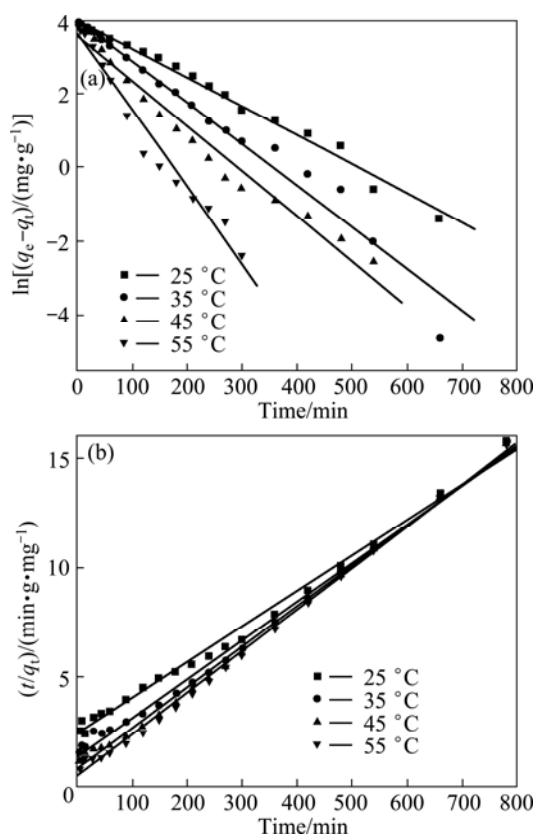


Fig. 7 Effect of temperature on kinetics for Glu removal with Mg-Fe-CLDH: (a) First-order kinetics model; (b) Pseudo second-order kinetics model

intraparticle diffusion is not the only rate-limiting step, but also other kinetic models may control the rate of adsorption, all of which may be operated simultaneously. Probably, the transport of Glu through the particle/sample interphase onto the pores of the particles, as well as adsorption on the available surface of the adsorbent, is responsible for the adsorption. The constants of k_p and C for the linear section are shown in Table 1. From Table 1, it can be noticed that the intraparticle diffusion coefficient k_p for the diffusion in the second region is decreased from 11.08 to 4.286 $\text{mg}/(\text{g}\cdot\text{h}^{0.5})$ with temperature increasing from 25 to 55 °C. The value of the intercept C provides information related to the thickness of the boundary layer, which increases with the increasing temperature in the second region. The

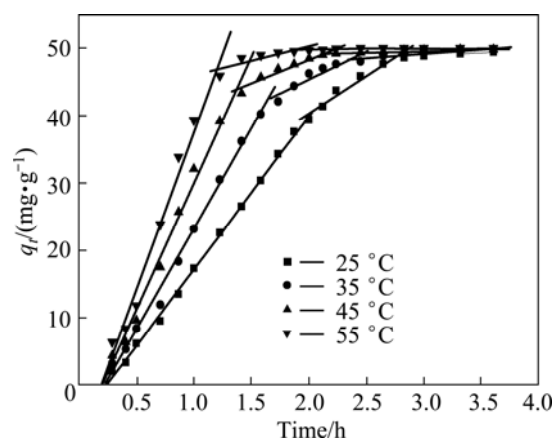


Fig. 8 Plot of intra-particle diffusion model of Glu onto Mg-Fe-CLDH at various temperature

increase of the intercept C suggests that the increasing temperature of the solution would reduce the rate of diffusion of Glu in the boundary layer. In other words, the surface diffusion becomes more important at a high temperature.

3.2.5 Adsorption isotherm

The adsorption isotherm is to describe how adsorbents interact with adsorbates in an adsorption system. For the liquid–solid system, adsorption isotherm equations usually use Langmuir equilibrium model and Freundlich equilibrium model. Langmuir's equation is used for estimating the maximum uptake values that cannot be reached in the experiments, which is based on the physical hypothesis that the maximum adsorption capacity consists of a monolayer adsorption, and that there are no interactions between adsorbed molecules. The empirical Freundlich equilibrium model is based on the fact that the adsorbent has a heterogeneous surface composed of different classes of adsorption sites, with adsorption on each class of sites following the Langmuir isotherm. It does not predict any saturation of the adsorbent by the adsorbates, thus infinite surface coverage is predicted mathematically, indicating multilayer adsorption of the surface. The linear form of Langmuir equilibrium model and the Freundlich equilibrium model are expressed as follows: [23,24]

Table 1 Kinetic parameters for adsorption experiments

Temperature/ °C	$q_{e,exp}/$ ($\text{mg}\cdot\text{g}^{-1}$)	Pseudo first-order			Pseudo second-order			Intraparticle diffusion		
		$q_{e,cal}/$ ($\text{mg}\cdot\text{g}^{-1}$)	k_1/h^{-1}	R^2	$q_{e,cal}/$ ($\text{mg}\cdot\text{g}^{-1}$)	$k_2/$ ($10^4\text{g}\cdot\text{mg}^{-1}\cdot\text{h}^{-1}$)	R^2	$C/$ ($\text{mg}\cdot\text{g}^{-1}$)	$k_p/$ ($\text{mg}\cdot\text{g}^{-1}\cdot\text{h}^{-0.5}$)	R^2
25	49.28	54.63	0.0079	0.9945	51.35	1.123	0.9963	18.054	11.08	0.9863
35	49.69	55.57	0.0113	0.9854	56.49	2.322	0.9971	28.89	8.228	0.9849
45	49.78	56.98	0.0122	0.9875	54.05	4.247	0.9975	34.39	6.906	0.9664
55	50.00	58.73	0.0209	0.9861	52.63	7.679	0.9983	41.63	4.286	0.9058

$$\frac{C_e}{q_e} = \frac{1}{K_L q_m} + \frac{C_e}{q_m} \quad (6)$$

$$\ln q_e = \ln k_f + \frac{1}{n} \ln C_e \quad (7)$$

where K_L is the equilibrium adsorption coefficient; q_m is the maximum adsorption capacity; C_e is the equilibrium concentration; k_f is the adsorption capacity at unit concentration; n is the adsorption intensity.

The fact was found that the Langmuir isotherm is a better model than the Freundlich isotherm according to their correlation coefficients ($R_L^2=0.9997$, $R_F^2=0.9102$), which may be due to the homogenous distribution of active sites on the Mg–Fe–CLDH surface. The better fitted Langmuir parameters are $q_m=84.034$ mg/g, $K_L=1.931$ L/mg. The constant K_L represents affinity between the adsorbent and adsorbate.

4 Conclusions

1) Mg–Fe–CLDH might be a potential material for the removal of Glu from aqueous solution. It was found that Glu could be removed effectively by optimizing experimental conditions with a removal rate of 96.2%. When competitive anions are co-existing, the removal rate of Glu increases in order of $\text{PO}_4^{3-} < \text{CO}_3^{2-} < \text{SO}_4^{2-} < \text{Cl}^- \ll \text{NO}_3^-$.

2) The kinetic and adsorption isotherm data fit well the pseudo second-order kinetic model and the Langmuir model respectively with good determination coefficient. The intraparticle diffusion model fits the data well, which suggests that the overall rate of diffusion of Glu can be described by two steps: film diffusion and particle diffusion.

References

- [1] JINAP S, HAJEB P. Glutamate: Its applications in food and contribution to health [J]. *Appetite*, 2010, 55: 1–10.
- [2] Fufeng Group. Expansion into consumer pack MSG [R]. Hong Kong: 2010.
- [3] MAO J Q, CHEN Q W, CHEN Y C. Three-dimensional eutrophication model and application to Taihu Lake, China [J]. *Journal of Environment Sciences*, 2008, 20(3): 278–284.
- [4] HONG S U, BRUENING M L. Separation of amino acid mixtures using multilayer polyelectrolyte nanofiltration membranes [J]. *Journal of Membrane Science*, 2006, 280(2): 1–5.
- [5] HAN M H, YUN Y S. Mechanistic understanding and performance enhancement of biosorption of reactive dyestuffs by the waste biomass generated from amino acid fermentation process [J]. *Biochemical Engineering Journal*, 2007, 36: 2–7.
- [6] BULUT Y, GOZUBENLI N, AYDIN H. Equilibrium and kinetics studies for adsorption of direct blue 71 from aqueous solution by wheat shells [J]. *Journal of Hazardous Materials*, 2007, 144(1–2): 300–306.
- [7] ORTHMAN J, ZHU H Y, LU G Q. Use of anion clay hydrotalcite to remove coloured organics from aqueous solutions [J]. *Separation Science Technology*, 2003, 31(1): 53–59.
- [8] POLLARD S J T, FOWLER G D, SOLLARS C J, PERRY R. Low-cost adsorbents for waste and wastewater treatment: A review [J]. *Science of the Total Environment*, 1992, 116(1–2): 31–52.
- [9] LI Feng, DUAN Xue. Applications of layered double hydroxides[M]//DUAN X, EVANS D G. *Structure and Bonding*. Springer International Publishing, 2006: 193–223.
- [10] LEGROURI A, LAKRAIMI M, BARROUG A, DE ROY A, BESSE J P. Removal of the herbicide 2,4-dichlorophenoxyacetate from water to zinc-aluminium-chloride layered double hydroxides [J]. *Water Research*, 2005, 39: 3441–3448.
- [11] CHAO Y F, LEE J J, WANG S L. Preferential adsorption of 2,4-dichlorophenoxyacetate from associated binary-solute aqueous systems by Mg–Al–NO₃ layered double hydroxides with different nitrate orientations [J]. *Journal of Hazardous Materials*, 2009, 165(1–3): 846–852.
- [12] WHO. Guidelines for drinking-water quality [M]. 2nd ed. Geneva: World Health Organization, 2003.
- [13] SILVERIO F, DOS REIS M J, TRONTO J, VALIM J B. Removal of aliphatic amino acids by hybrid organic-inorganic layered compounds [J]. *Applied Surface Science*, 2007, 253(13): 5756–5761.
- [14] REINHOLDT M X, KIRKPATRICK R J. Experimental investigations of amino acid-layered double hydroxide complexes: Glutamate-hydrotalcite [J]. *Chemistry of Materials*, 2006, 18(10): 2567–2576.
- [15] TURK T, ALP I, DEVECI H. Adsorption of as (V) from water using Mg–Fe-based hydrotalcite (FeHT) [J]. *Journal of Hazardous Materials*, 2009, 171(1–3): 665–670.
- [16] BARTH A. Infrared spectroscopy of proteins: Review [J]. *Biochimica et Biophysica Acta: Bioenergetics*, 2007, 1767(9): 1073–1103.
- [17] CAVANI F, TRIFIRO F, VACCARI A. Hydrotalcite-type anionic clays: Preparation properties and application [J]. *Catalysis Today*, 1991, 11: 173–301.
- [18] LV L, HE J, WEI M, DUAN X. Kinetic studies on fluoride removal by calcined layered double hydroxides [J]. *Industrial and Engineering Chemistry Research*, 2006, 45(25): 8623–8628.
- [19] LV L, HE J, WEI M, EVANS D G, DUAN X. Factors influencing the removal of fluoride from aqueous solution by calcined Mg–AlCO₃ layered double hydroxides [J]. *Journal of Hazardous Materials*, 2006, 133: 119–128.
- [20] NI Z M, XIA S J, WANG L G, XING F F, PAN G X. Treatment of methyl orange by calcined layered double hydroxides in aqueous solution: Adsorption property and kinetic studies [J]. *Journal of Colloid and Interface Science*, 2007, 316: 284–291.
- [21] HO Y S, MCKAR G A. Comparison of chemisorption kinetic models applied to pollutant removal on various sorbents [J]. *Process Safety and Environment Protection*, 1998, 76(4): 332–340.
- [22] WEBER W J, MORRIS J C. Kinetics of adsorption on carbon from solution [J]. *Journal of the Sanitary Engineering Division, American Society of Civil Engineers*, 1963, 89: 31–59.
- [23] WU F C, TSENG R L. Liquid–solid phase countercurrent multi-stage adsorption process for using the Langmuir equation [J]. *Journal of Hazardous Materials*, 2008, 155: 449–458.
- [24] TSENG R L, WU F C. Inferring the favorable adsorption level and the concurrent multi-stage process with the Freundlich constant [J]. *Journal of Hazardous Materials*, 2008, 155: 277–287.

Mg-Fe-CLDH 对模拟谷氨酸废水的吸附分离

焦飞鹏, 帅丽, 于金刚, 蒋新宇, 陈晓青, 杜邵龙

中南大学 化学化工学院, 长沙 410083

摘要: 采用共沉淀法合成 Mg 与 Fe 摩尔比为 3:1 的层状双金属氢氧化物(Mg-Fe-LDH), 然后在 500 °C 下煅烧 6 h 得到煅烧双金属氢氧化物(Mg-Fe-CLDH)。分析 Mg-Fe-CLDH 与 Mg-Fe-LDH 对谷氨酸的吸附性能, 研究溶液 pH、谷氨酸初始浓度、共存阴离子及温度等因素对吸附效果的影响, 并对其吸附过程的动力学和热力学过程进行研究。结果表明: Mg-Fe-CLDH 对谷氨酸的吸附效果很好, 吸附率在优化条件下达到 99.9%; 吸附动力学符合准一级动力学方程, 平衡吸附等温线很好地符合 Langmuir 方程。颗粒内扩散模型能很好地描述吸附动力学过程。颗粒内扩散模型拟合结果显示, 颗粒内扩散不是唯一的反应速率控制步骤。

关键词: 煅烧型; 层状双金属氢氧化物; 谷氨酸; 吸附

(Edited by Hua YANG)